STUDYING METABOLISM IN A MODEL ANIMAL

USING AN ATP SENSOR PROTEIN

By

Jose Alberto Soto

A capstone project submitted for Graduation with University Honors

May 5, 2021

University Honors
University of California, Riverside

APPROVED

Dr. Morris F. Maduro
Department of Molecular, Cell, and Systems Biology

Dr. Richard Cardullo, Howard H Hays Jr. Chair, University Honors

ABSTRACT

The nematode *Caenorhabditis elegans* is a powerful model system to study fundamental biochemical processes such as those in metabolism. Food digestion is a crucial component of human biology, and studying models for nutrient breakdown and energy storage will help shed light on fundamental questions that are applicable to all living systems, including humans. This project involves identifying determinants of metabolic rates by studying the function of the intestine in wild-type and mutant *C. elegans* animals. A key component of metabolism in all living cells is the availability of adenosine triphosphate, or ATP, the main source of chemical energy transfer. The Maduro lab has found that partially compromised specification of gut in the embryo leads to increased fat storage in surviving adults. They previously identified genes whose expression changes in the gut of these strains. Two of these genes are *fstr-1* and *fstr-2*. In wild-type animals *fstr-2* is expressed, and in specification- compromised animals (e.g. the strain MS404), it is *fstr-1* that is expressed. The two genes make related proteins that may be important for import of food into gut cells. We hypothesize that these strains differ in their metabolism, such that the concentration of ATP in the living animals would be different. Using an engineered protein that responds to endogenous ATP levels in living cells through Förster resonance energy transfer, or FRET, we measured steady-state levels of ATP in the living animals. Our results suggest that the ATP sensor protein produces detectable signal that shows signal differences, as expected, in control and genetic backgrounds that influence ATP levels. We are continuing use this sensor in *C. elegans* and use it to measure metabolism in the various mutant backgrounds.

ACKNOWLEDGEMENTS

I would like to acknowledge my faculty mentor Dr. Morris F Maduro for all his support throughout this whole University Honors capstone project and for his mentorship in the RISE and MARC U STAR program as well. Without his guidance I would not be the student and researchers I am today and I am extremely excited to carry on what I have learned into my graduate school PhD program. I also acknowledge my lab members Gina Maduro, Ivan Dimov, and Madeline Rivera for their teamwork and collaborative learning environment they all provided. In addition I would like to acknowledge University Honors for providing all the resources necessary to carry on this project and for providing excellent research preparation with other Honors faculty. We also gratefully acknowledge Gladstone Institutes and Ken Nakamura, M.D., Ph.D for providing the plasmids used in this study, and acknowledge the contribution of Hiromi Imamura, Ph.D., Professor, Kyoto University, for the generation of the original ATP biosensor (Imamura et al., 2009). This project is supported by Award Number T34GM062756.

Table of Contents

INTRODUCTION

The nematode *Caenorhabditis elegans* (*C. elegans*) is used for studying many biological problems. The *C. elegans* intestine is a major site of the generation and storage of chemical energy. Adenosine triphosphate (ATP) is a major molecule involved in energy transfer, hence regulation of intracellular ATP levels is a critical aspect of metabolism. Metabolism is a series of chemical processes that occurs within living organisms in order to sustain life. ATP in *C. elegans* has been measured using different *in-vivo* and *in-vitro* methods. Previous methods of measuring ATP included bioluminescence and enzyme-based assays (Palikaras & Tavernarakis, 2016)The benefit of using the bioluminescence approach is that is allows for accurate concentration measurements of free ATP throughout the entire body of *C. elegans* animals and in different tissues. However, these biochemical methods cannot be performed on living animals/cells as the process requires the tissue to be frozen and dissolved in a mixture of solutions to measure ATP concentrations *in-vitro* (Palikaras & Tavernarakis, 2016). The limitation of the bioluminescence approach in *C. elegans* is the lack of resolution of measuring ATP at the cellular level that could instead be achieved with an *in-vivo* approach. Recently, ATP sensor proteins have been used to indirectly measure ATP levels in living cells (Zhang et al., 2018). These sensors are derived by inserting the ε subunit of the bacterial F_0F_1-ATP synthase between two fluorescent protein domains, allowing detection of protein bound to ATP by Förster Resonance Energy Transfer, or FRET (Imamura et al., 2009). A previous ATP FRET sensor was used to measure ATP in the muscle cells of the pharynx of *C. elegans* (Tsuyama et al., 2013). It is known the muscle cells tend to have higher concentrations of ATP due to a constant requirement for energy (Tsuyama et al., 2013). In our experiment we test the intestinal expression of a similar FRET-based ATP sensor derived from the green/red fluorochrome pair Clover/mApple (Figure 1A) in a location within the organism where energy is both harvested and stored. This experiment will develop

another method of measuring steady-state ATP levels in the *C. elegans* system and would be accessible to many labs, requiring minimal training. In addition, through the use of this ATP FRET sensor protein, we can study what genes affect ATP levels and ultimately what genes are responsible in metabolism.

Background & Design

Figure 1

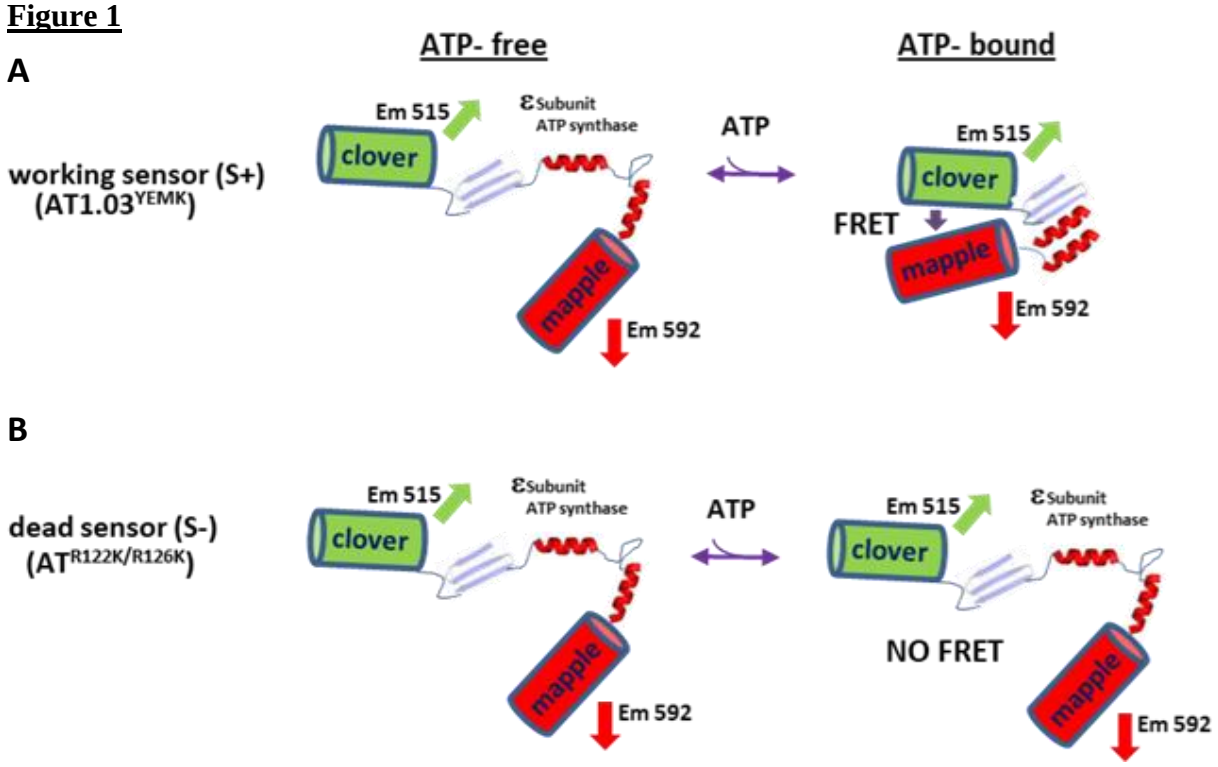

(A). ATP FRET sensor (+), $AT^{1.03YEMK}$ design and construct. (B) Dead sensor (-), $AT^{R122K/R126K}$ design and construct. Clover fluorescent protein indicated by the green cylinder (left and top). Emission of 515nm (green light) when excited. mApple fluorescent protein indicated by red cylinder (right and bottom). Emission of 592nm when excited (red light). ε subunit ATP synthase indicated by red helix tether between Clover and mApple. A & B displays sensor's reaction to addition of ATP.

The recombinant protein that has been engineered for this project's sensor (Figure 1A) consists of two fluorescent proteins, Clover and mApple, which are present on either side of an ATP binding domain (Mendelsohn et al., 2018). This sensor was previously used by Mendelsohn (2018) where they performed ATP measurements in cultured cells, whereas this experiment

implements the FRET sensor into *C. elegans*, specifically in the gut cells. Exciting the Clover portion of the protein with blue light gives green emission, while exciting the mApple portion of the protein with green light gives red emission. This overlap of green emission from the Clover protein (donor) and green excitation of the mApple protein (acceptor) is what causes the FRET interaction (Mendelsohn et al., 2018). When an ATP molecule binds to the ATP binding domain in the sensor, the binding brings the fluorescent proteins closer together, within 10nm of each other, allowing for FRET signal to occur, where blue light absorbed by the Clover fluorescent protein ends up emitted as green light which then directly excited the mApple fluorescent protein to produce red light (Mendelsohn et al., 2018). By exciting with blue light and measuring the amount of red light produced we can measure the amount of FRET levels by taking ratio of the amount of FRET signal over the amount of sensor protein (Mendelsohn et al., 2018). Therefore, the amount of red emission from the sensor protein, due to blue excitation, indirectly measures the fraction of protein that bound to ATP. The excitation/emission of the Clover or mApple portions can be detected from the sensor protein regardless of its interaction with ATP. The detection from mApple produced a much higher signal-to-noise ratio than Clover because of lower red autofluorescence in the gut. Thus, it is ideal to use mApple signal to detect the amount of sensor present in the gut.

In order to use this sensor within the intestine of *C. elegans* the proper controls are required to ensure the effective measurement of ATP. To confirm that the signal detected from the sensor is relevant to the interaction of ATP binding to the ATP binding domain, we tested a dead version of the sensor (Dead sensor (-), $AT^{R122K/R126K}$) with an inactive ATP binding domain against the normal sensor, ATP FRET sensor (+), $AT^{1.03YEMK}$ (Figure 1B) (Mendelsohn et al., 2018). If the normal sensor does not produce higher signal compared to the dead sensor, then that

would suggest, the normal sensor's signal is not relevant to the active ATP binding domain. Provided that the normal sensor does in fact produce significantly higher signal than the dead sensor, to ensure that the normal sensor is capable of measuring changes in ATP levels, we tested wild-type against other strains, previously studied by others, that affect ATP concentrations within *C. elegans* (Figure 6). This genetic backgrounds include *daf-2* and *atp-3,* which we introduced by RNAi knockdown, and the *daf-16* strains. Detection of higher signal compared to the dead sensor, and effective measurements in changes in ATP would suggest that the sensor is capable of measuring steady-state ATP levels within the intestine of *C. elegans* and could be used to study differences in metabolism in different genetic backgrounds.

Experimental Setup

Strain and Sensor Preparation:

Expression of this sensors have been localized to the anterior of the gut in *C. elegans* under regulation of the *pept-1* promoter (Mendelsohn et al., 2018; Nehrke, 2003). The transgenes containing the DNA coding for the sensors was integrated into animal's genome by exposure to ionizing radiation after microinjection of the transgene. This integration process allows for stable expression of the sensor across a population of *C. elegans* that can be propagated in all of the progeny. The sensor can then be introduced into other mutant strains by performing a cross between female hermaphrodites and male *C. elegans.*

Imaging Set:

Figure 2

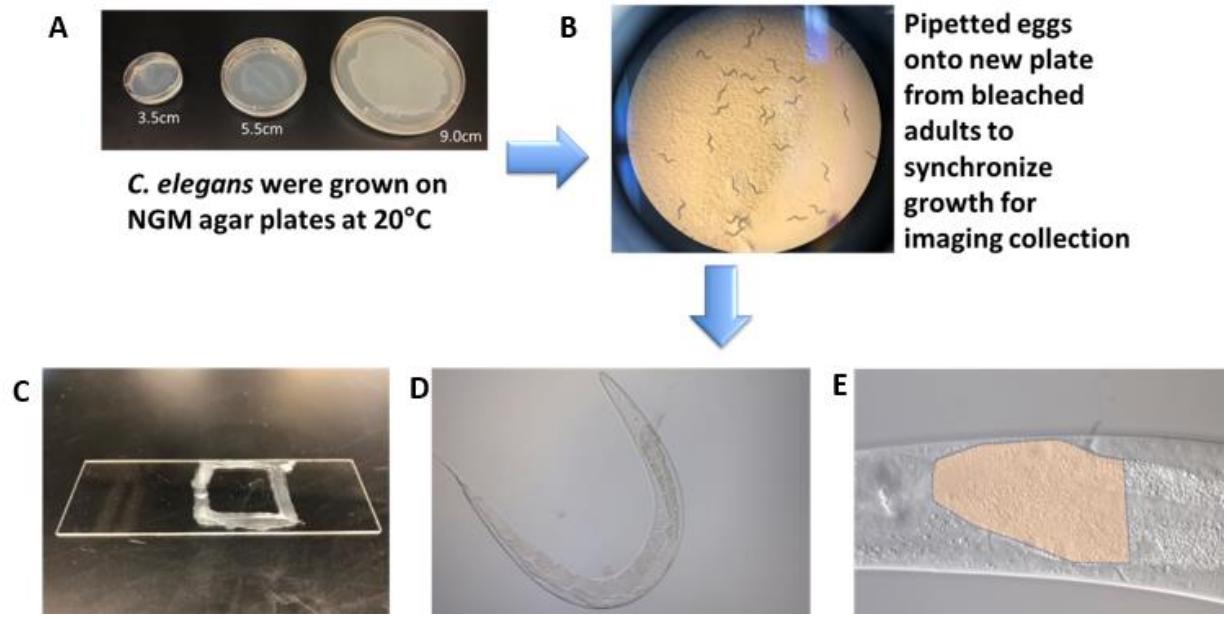

(A) Small (3.5cm), medium (5.5cm), and large (9.0cm) agar plates used for growth of bacteria and strains. (B) Image of day-1 adults on medium plate obtained from low-low dissection light microscope. (C) Glass slide with day-1 adults ready to be moved to microscope. (D) Body of C. elegans imaged using 40x objective. (E) *C. elegans* imaged using 63x objective, with anterior of gut highlighted in orange hue representing localization of the sensor's fluorescent expression.

Figure 3

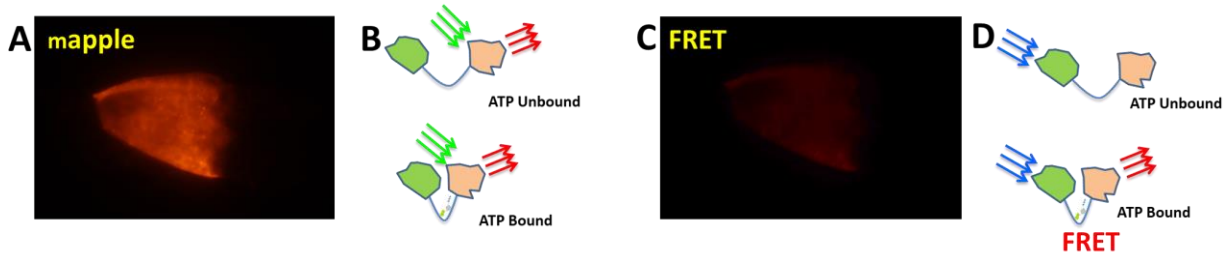

(A) ATP FRET sensor (+), AT$^{1.03YEMK}$ mApple signal. (B) Schematic demonstrating that A measures amount of sensor present independent of ATP binding. (C) ATP FRET sensor (+), AT$^{1.03YEMK}$ FRET signal. (D) Schematic demonstrating that C measures signal of mApple dependent on ATP binding.

As a control, we solely imaged day-1 to day-2 adults in order to keep the age and stage of the strains' growth consistent for data collection (Figure 2B). In order to obtain a large population of *C. elegans* to image, we performed a bleaching procedure that isolates the embryos from adults and pipetted those embryos onto agar plates and waiting approximately 2-3 days for imaging. For data collection, *C. elegans* were mounted on a glass slide to imaged fluorescence (Figure 2C & D). Using a microscope camera adapter and a mercury (Hg) fluorescent lamp along with filter cubes in the light microscope, the Hg lamp produces a white-like light that passes through a filter cube transmitting the correct wavelength of light for excitation of the sensor protein. Two images focusing in the anterior of the gut (Figure 2E) were taken in rapid succession as to mitigate fluorescent variability (Sinnecker et al., 2005). The first image measured the emission of the mApple protein from the sensor to determine the total amount of sensor present (Figure 3A). This was done by exciting directly mApple with green light to produce red light (Figure 3B). The second image measured emission of the mApple protein due to the initial excitation of Clover (Figure 3C). This red signal was due to excitation of Clover by blue light (Figure 3D). The pixel values from the images was used to generate the FRET data. We collected the ratio of FRET over amount of sensor present to compare differences in energy levels across strains. The first test was a comparison of the normal sensor to the dead sensor. The second test was an RNAi manipulation of metabolism. Wild-type *C. elegans* were compared to *daf-2* mutants that are known to have positive effects on energy levels and metabolism, versus *atp-3* mutants that inhibit the production of ATP (Dillin et al., 2002). With these two controls, we proceeded to perform initial tests of the sensor in different genetic backgrounds that our lab is currently researching and one that has also been previously studied by others, *clk-1*, known to have a positive effect on ATP levels at later adult stages (Braeckman et al.,1999). The mutant

strains, *nhr-156* and *fstr-1,2*, mutates a newly-discovered transcription factor that apparently increases synthesis of fat storage and produce novel proteins that may have a role in regulating food intake, respectively.

RESULTS

Normal Sensor and Dead-Kinase Sensor

Figure 4

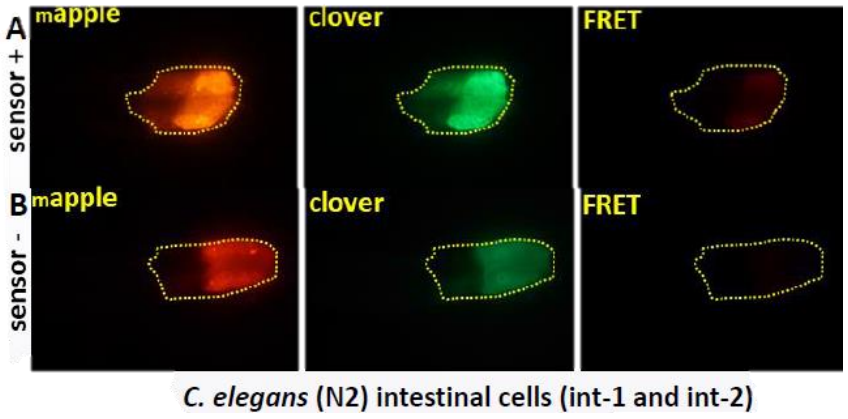

(A) ATP FRET sensor (+), $AT^{1.03YEMK}$ signal including mApple, Clover, and FRET signal due to initial Clover excitation

(B) Inactive sensor (-), $AT^{R122K/R126K}$ signal including mApple, Clover, and FRET signal due to initial Clover excitation

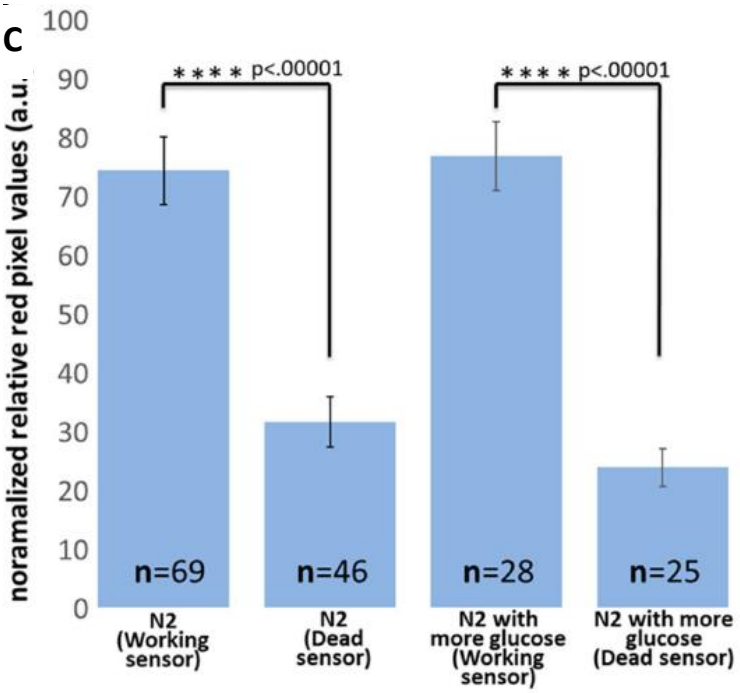

(C) Normalized relative red pixel values (a.u) from *C. elegans* with sensor (+) and sensor (-) grown on normal and increased glucose levels.

N_2 represents the wild-type strain.

n represents the population values

"Working sensor" represents the normal sensor with the active ATP binding domain.

"Dead sensor" represent the sensor with the inactive ATP binding domain.

Error bars display the standard error values.

Statistical differences display p-values from two sided t-test

Day-1 adults of N_2 strains with the normal sensor and N_2 strains with the kinase-dead sensor were imaged for their fluorescent signal as seen in Figure 4. mApple was imaged (Figure 4A) in a range above 100 red pixel values to measure the amount of sensor in the image. The Clover signal (Figure 4B). Clover was not used to measure the amount of sensor to prevent any unnecessary FRET signal The FRET image (Figure 4C) is the signal dependent on ATP binding to the sensor. Images were taken in pairs and then moved into Adobe Photoshop to highlight the selected area of fluorescence and measure the red pixel values provided from the histogram feature within the software. The average red pixel values were then moved onto a spreadsheet to then calculate the ratio of average red pixel values (mApple/FRET). The average of the ratio of the averages (mean value of mApple/FRET) was then normalized for visual representation as seen in Figure 4C. After normalization, N_2 with the working sensor was measured at 72.02 ± 5.61 and 74.41 ± 5.62 with normal and more glucose respectively. N_2 with the dead sensor was measured at 30.51 ± 4.18 and 22.99 ± 3.09 with normal and more glucose respectively. Values for $\pm$ were obtained from error bars indicating the standard error values after normalization. In both experimental cases the working sensor and dead sensor were found statistically different at $p < 0.00001$. (a.u. = arbitrary units)

Automatic Analysis of Images

Figure 5

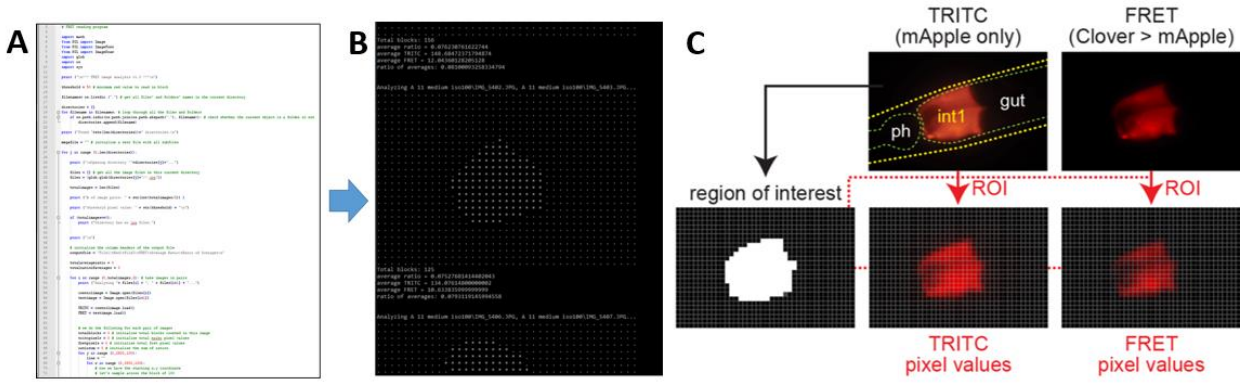

(A) Sample of Python script created by Dr. Maduro for the FRET analysis. When the script is run by the user, the program is displayed on the computer screen as shown in image B. (C) Image displaying the function of the script. The program highlights the region of interest int-1, between the pharynx (ph) and the rest of the gut, in the image pairs of TRITC and FRET if the pixel values is above 50. The program then measures the red pixel values in the image pairs.

In order to standardize and automate the method of analyzing the image analysis portion of the project, Dr. Maduro created a python script to handle the analysis process (Figure 5A). The script can complete the tasks performed manually in an equal manner, but on a more rapid scale of approximately 100 images per minute (Figure 5B). Our initial data collected manually, served as a control for this program to ensure that the data being produced by the software was representative of the data that one can measure by hand (Figure 5C). This system outputs the image number of each image pair, the average value of TRITC, the average FRET, the average ratio, the ratio of averages, and the average ratio of averages.

Measuring Changes in ATP Levels Using ATP Sensor

Figure 6

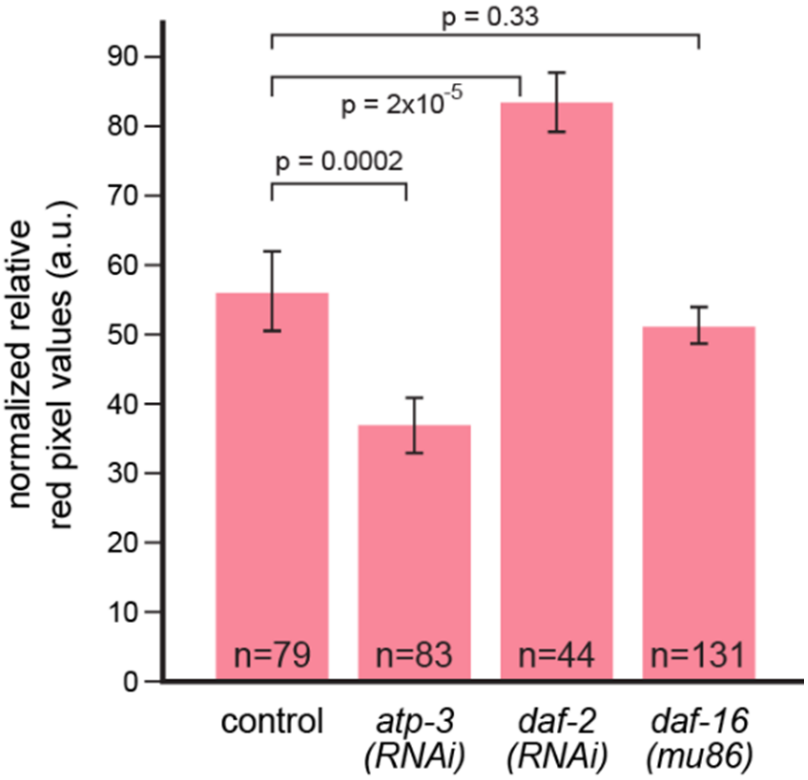

Normalized relative red pixel values (a.u) from control (empty vector), *atp-3* (RNAi), *daf-2* (RNAi), and *daf-16* mutant.

n represents the population values

Error bars display the standard error values.

Statistical differences display p-values from two sided t-test

Day-1 adults with the working sensor fed with HTT115 bacteria carrying the empty vector, *daf-2*, and *atp-3* RNAi sequences were imaged for their fluorescent signal using the same methods mentioned previously. Images were then analyzed using the newly developed python script (Figure 5). Data was then moved to a spread sheet and then visually represented in Figure 6 using normalized values of the fluorescent signal. After normalization, the control (empty vector), *atp-3*, *daf-2*, and *daf-16* strains were measured at 55.94 ± 4.15, 36.75 ± 4.04, 83.21 ± 4.31, and 51.12 ± 2.71 respectively. Values for ± were obtained from error bars indicating the standard error values after normalization. Statistical comparison between control and *atp-3*, control and *daf-2*, and control and *daf-16* were measured with p values 0.0002, $2x10^{-5}$, and 0.33 respectively. (a.u. = arbitrary units)

Initial Comparisons of ATP Across Strains of Interest

Figure 7

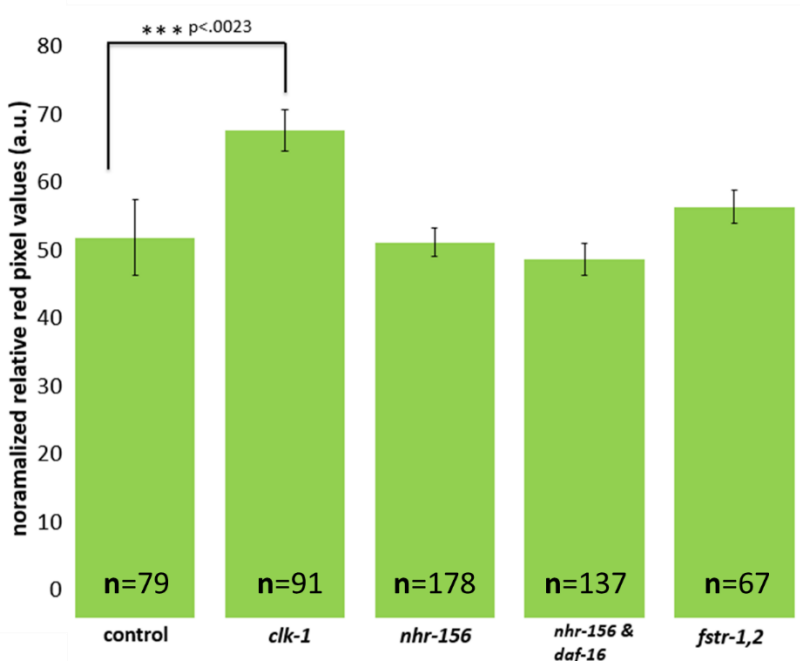

Normalized relative red pixel values (a.u) from control, *clk-1*, *nhr-156*, *nhr-156* & *daf-16*, and *fstr-1,2*

n represents the population values

Error bars display the standard error values.

Statistical differences display p-values from two sided t-test

ATP levels from four different genetic backgrounds were measured using the normal sensor while the control data from Figure 6 was used for control. Images were then analyzed using the python script (Figure 5). Figure 6 visually represents normalized values of the fluorescent signal. After normalization, *clk-1*, *nhr-156*, *nhr156* & *daf-16*, and *fstr-1,2* were measured at 71.68 ± 3.06, 55.21 ± 2.07, 52.75 ± 2.38, and 60.85 ± 3.92 respectively. Statistical comparison between control and *clk-1* were measured with p value 0.0023. Values for ±, error bars, and p value were obtained using same methods previously mentioned. (a.u. = arbitrary units)

DISCUSSION

Working with this sensor required many controls in order to properly determine the sensor's ability to measure ATP. Image pairs were obtained from a glass slide with immobile *C.*

elegans containing the transgene. Anesthesia could not be used to secure the worms in place for imaging as the anesthetic affects ATP levels within the animal. Therefore, careful preparation of glass slide was required for no movement in order to obtain quality image pairs. Initial tests with the sensor revealed varying and inconsistent signal while trying to use the Clover protein to measure the amount of sensor. However, using the mApple protein to measure the amount of signal mitigated that the variance in fluorescence. Thus, for all data collection and representation the mApple protein was used for both the measurement of total amount of sensor and for FRET signal.

Normal Sensor and Dead-Kinase Sensor

The normal kinase sensor in N_2 showed significantly higher signal compared to the dead-kinase sensor in N_2 in both normal glucose levels and increased glucose levels. This suggests that the sensor's signal is relevant to the functioning ATP binding domain in the normal sensor. Therefore, there is increased signal when ATP binds to the domain bringing the two fluorescent molecules, Clover and mApple, within the 10nm range to allow for stronger FRET interaction. Due to the inactive domain in the dead sensor, there was little to no signal and is possibly the base or background signal of the sensor. With this control completed, we could confidently test the sensor's capability of measuring changes in ATP in different backgrounds.

Automatic Analysis of Images

Using the python script rapidly sped up the process of analyzing the images allowing for more time to be invested into collected quality images for data collection. The script was reliably producing data in an equal manner compared to the original manual analysis of the images using Adobe Photoshop. While, the manual analysis technique was no longer used for the collection of the FRET data, the initial experiment served as a control for the script so we could confidently

use the software moving forward. The script not only had an advantage through its faster processing speed, but we had the ability to download the software on any computer device in the lab to use on the image pairs. The program was activated using the Command Prompt application on Windows computers where the program would perform its tasks on any folder within the same directory as the Python script.

M*easuring Changes in ATP Levels Using ATP Sensor*

We examined three different genetic conditions to determine if the sensor was capable of producing similar relative ATP levels as previously determined by others (Figure 6). RNAi mediated knockdown of the nuclear-encoded ATP synthase subunit gene *atp-3* by RNAi results in a decrease of 60-80%, and knockdown of *daf-2*, resulted in an increase of 100-200% in biochemical ATP levels in whole animals, depending on their age (Dillin et al., 2002). In contrast, the mutation of *daf-16* produced little or no change in ATP levels (Braeckman et al., 1999; Dillin et al., 2002). Mutation of *daf-2* produced a modest increase in muscle ATP levels after several days, measured by A similar FRET-based ATP sensor, ATeam (Wang et al., 2019). As shown in Figure 6, our results were qualitatively similar. However, the differences seen with the sensor, while statistically significant, are of smaller magnitude, i.e. only a 40% decrease in *atp-3*(RNAi) and a 50% increase in daf-2(RNAi). Conservatively, therefore, an *in-vivo* ATP biosensor is best used to compare relative free ATP levels across genotypes and conditions, and not to directly infer actual biochemical changes. Our results suggest that even with a modest low-cost fluorescence setup, an *in-vivo* ATP FRET reporter can be a useful way to measure aspects of metabolic state in the *C. elegans* intestine. Improvements in expression of the reporter and the use of confocal microscopy are likely to further increase the usefulness of this system.

Initial Comparisons of ATP Across Strains of Interest

We performed initial tests of the sensor in four different strains of interest in our lab to compare relative free ATP levels. Mutation of *nhr-156*, and *nhr-156* with *daf-16* produced little to no change in ATP levels, while mutation of *fstr-1,2* indicates a more slight change in ATP levels but not within statistical significance. However, mutation of *clk-1* resulted in an increase of 25% in sensor signal. The *clk-1* mutant is known to have similar levels of ATP with young N_2 adults and higher levels of ATP as the *C. elegans* age and get closer to the end of their lifespan (Braeckman et al., 1999, 2002). Our results suggest, that there may be a slightly modest increase in ATP levels within the intestinal cells in *clk-1* mutants compared to N_2 even in early adulthood. However, the maintenance of higher ATP levels in *clk-1* strains remains to be tested in future experiments that could incorporate improved expression of the sensor and confocal microscopy.

METHODS AND MATERIALS

Plasmids and Integration Procedure

The plasmid obtained in this experiment that contain the normal and kinase-dead versions of the novel Clover-ATP-mApple fusion protein were from a group at the University of California Berkeley (Mendelsohn et al., 2018). These were used for PCR and Gibson assembly to fuse 1407 bp of the *pept-1* promoter to the sensor coding region and the 3'UTR of *unc-54* from vector pPD95.67. We made transgenic *unc-119*(ed4) mutants for the *pept-1*-driven sensor and an *unc-119*(+) rescue plasmid by microinjection. Arrays were integrated by exposure to gamma radiation to produce double stranded breaks within the DNA of *C. elegans* whereby we could then capture the rare event of the extra chromosomal array being integrated into the genome seen in the F_2 generation. This generated the MS2495 strain carrying irIs158 (normal sensor) and MS2499 carrying irIs162 (kinase-dead sensor).

Strain Maintenance and Preparation

N_2 strains carrying the normal sensor and N_2 carrying the kinase-dead sensor were grown and maintained on NGM agar plates with *E. coli* OP50. RNAi was performed by feeding of the HT115 bacteria carrying the empty vector, *daf-2* or *atp-3* sequences using standard methods (Kamath and Ahringer, 2003). Population of strains were bleached and then pipetted onto an agar plate to synchronize growth of strains from the embryo stage for imaging. *C. elegans* were maintained at 20°C until day-1 adulthood (non-gravid) was reached. Strains were then mounted onto a glass slide, where movement would be restricted, and moved to the microscope for fluorescent imaging.

Imaging of Fluorescent Signal

The anterior intestines of 1- to 2-day old adults were imaged on an Olympus BX-51 upright epifluorescence microscope equipped with a 100W mercury arc lamp and Canon EOS 77D camera with LMScope Cmount adapter. The mApple fluorescent protein was imaged using a Chroma 31002 TRITC filter set. For FRET imaging we combined the HQ500/20x exciter and Q515lp beam splitter from a Chroma 41029 YFP filter set with a 635/20 emission bandpass filter (a gift from Dr. David Carter, UCR Microscopy Core). To account for photobleaching of fluorescent signal and to minimize variability in fluorescence intensity, images for a set of experiments were acquired within a short time using the same mercury bulb and settings.

Manual Analysis of Images

Images of size 2656×3984 pixels were taken at ISO 100 and ¼ sec exposure and saved in JPG format using Canon Digital Photo Professional. In our first studies, we opened the two images into Adobe Photoshop and used the control TRITC image to identify the fluorescent

region of interest. We would then extract the red pixel values of this region from both images using the histogram feature provided within the program.

Automatic Analysis of Images

Images were taken and saved as mentioned previously. The manual analysis served as a control for our automatic analysis. We developed a Python script to process image pairs automatically (available at https://github.com/MaduroMF/FRETcalc/releases/tag/1.0). The script subdivides the first image into 100×100 pixel blocks, and if the average red pixel value of a block is higher than a background of 50, then the average red pixel values are recorded from the same block between both the control (TRITC) and FRET images. For each image pair the program computes both the average of the ratios obtained across the regions of interest, as well as the ratio of the average pixel values. For the histograms shown in Figures 6 and 7, the ratio of the average red pixel values was used to compute the means, standard error, and p values using a two-sided t-test. The pixel ratio (r) values were scaled for the histogram by computing (r-0.04)/0.04*100. The subtracted ratio of 0.04 was obtained from measurements of background FRET from a kinase-dead version of the sensor.

REFERENCES

Braeckman, B. P., Houthoofd, K., De Vreese, A., & Vanfleteren, J. R. (1999). Apparent uncoupling of energy production and consumption in long-lived Clk mutants of Caenorhabditis elegans. *Current Biology, 9*(9), 493–497.

Braeckman, B. P., Houthoofd, K., De Vreese, A., & Vanfleteren, J. R. (2002). Assaying metabolic activity in ageing Caenorhabditis elegans. *Mechanisms of Ageing and Development, 123*(2–3), 105–119.

Dillin, A., Hsu, A.L., Arantes-Oliveira, N., Lehrer-Graiwer, J., Hsin, H., Fraser, A.G., Kamath, R.S., Ahringer, J., Kenyon, C., 2002. Rates of behavior and aging specified by mitochondrial function during development. Science 298, 2398-2401.

Imamura, H., Nhat, K.P., Togawa, H., Saito, K., Iino, R., Kato-Yamada, Y., Nagai, T., Noji, H., 2009. Visualization of ATP levels inside single living cells with fluorescence resonance energy transfer-based genetically encoded indicators. PNAS USA 106, 15651-15656. DOI: https://doi.org/10.1073/pnas.0904764106 | PMID: 19720993.

Kamath, R.S., Ahringer, J., 2003. Genome-wide RNAi screening in Caenorhabditis elegans. Methods 30, 313-321. DOI: https://doi.org/10.1016/s1046-2023(03)00050-1 | PMID: 12828945. 7/30/2020 - Open Access

Mendelsohn, B.A., Bennett, N.K., Darch, M.A., Yu, K., Nguyen, M.K., Pucciarelli, D., Nelson, M., Horlbeck, M.A., Gilbert, L.A., Hyun, W., Kampmann, M., Nakamura, J.L., Nakamura, K., 2018. A high-throughput screen of real-time ATP levels in individual cells reveals mechanisms of energy failure. PLoS Biology 16, e2004624. DOI: https://doi.org/10.1371/journal.pbio.2004624 | PMID: 30148842.

Nehrke, K., 2003. A reduction in intestinal cell pHi due to loss of the Caenorhabditis elegans Na+/H+ exchanger NHX-2 increases life span. Journal of Biological Chemistry 278, 44657-44666. DOI: https://doi.org/10.1074/jbc.m307351200 | PMID: 12939266.

Palikaras, K., & Tavernarakis, N. (2016). Intracellular assessment of ATP levels in Caenorhabditis elegans. *Bio Protoc*, *6*(23), e22048.

Sinnecker, D., Voigt, P., Hellwig, N., & Schaefer, M. (2005). Reversible photobleaching of enhanced green fluorescent proteins. *Biochemistry*, *44*(18), 7085–7094.

Tsuyama, T., Kishikawa, J., Han, Y.W., Harada, Y., Tsubouchi, A., Noji, H., Kakizuka, A., Yokoyama, K., Uemura, T., Imamura, H., 2013. In vivo fluorescent adenosine 5'-triphosphate (ATP) imaging of Drosophila melanogaster and Caenorhabditis elegans by using a genetically encoded fluorescent ATP biosensor optimized for low temperatures. Analytical Chemistry 85, 7889-7896. DOI: https://doi.org/10.1021/ac4015325 | PMID: 23875533.

Wang, H., Webster, P., Chen, L., Fisher, A.L., 2019. Cell-autonomous and non-autonomous roles of daf-16 in muscle function and mitochondrial capacity in aging C. elegans. Aging 11, 2295-2311. DOI: https://doi.org/10.18632/aging.101914 | PMID: 31017874.

Zhang, J., Han, X., Lin, Y., 2018. Dissecting the regulation and function of ATP at the single-cell level. PLoS Biology 16, e3000095. DOI: https://doi.org/10.1371/journal.pbio.3000095 | PMID: 30550559.